Ocean Modeling in an Eddying Regime

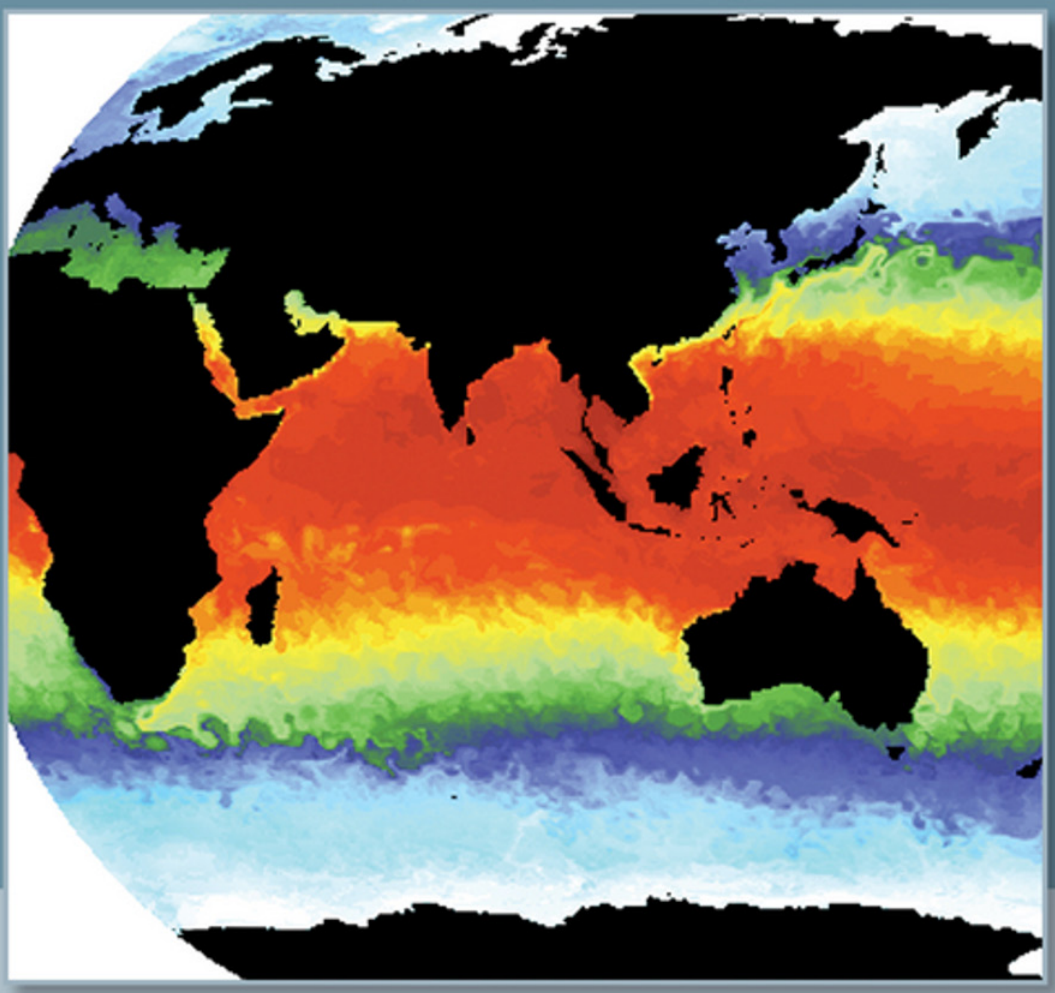

Matthew W. Hecht and Hiroyasu Hasumi,
Editors

AGU

Geophysical Monograph Series

Including
IUGG Volumes
Maurice Ewing Volumes
Mineral Physics Volumes

142 **Disturbances in Geospace: The Storm-Substorm Relationship** *A. Surjalal Sharma, Yohsuke Xamide, and Gurbax S. Lakhima (Eds.)*

143 **Mt. Etna: Volcano Laboratory** *Alessandro Bonaccorso, Sonia Calvari, Mauro Coltelli, Ciro Del Negro, and Susanna Falsaperla (Eds.)*

144 **The Subseafloor Biosphere at Mid-Ocean Ridges** *William S. D. Wilcock, Edward F. DeLong, Deborah S. Kelley, John A. Baross, and S. Craig Cary (Eds.)*

145 **Timescales of the Paleomagnetic Field** *James E. T. Channell, Dennis V. Kent, William Lowrie and Joseph G. Meert (Eds.)*

146 **The Extreme Proterozoic: Geology, Geochemistry, and Climate** *Gregory S. Jenkins, Mark A. S. McMenamin, Christopher P. McKay, and Linda Sohl (Eds.)*

147 **Earth's Climate: The Ocean–Atmosphere Interaction** *Chunzai Wang, Shang-Ping Xie, and James A. Carton (Eds.)*

148 **Mid-Ocean Ridges: Hydrothermal Interactions Between the Lithosphere and Oceans** *Christopher R. German, Jian Lin, and Lindsay M. Parson (Eds.)*

149 **Continent-Ocean Interactions Within East Asian Marginal Seas** *Peter Clift, Wolfgang Kuhnt, Pinxian Wang, and Dennis Hayes (Eds.)*

150 **The State of the Planet: Frontiers and Challenges in Geophysics** *Robert Stephen John Sparks, and Christopher John Hawkesworth (Eds.)*

151 **The Cenozoic Southern Ocean: Tectonics, Sedimentation, and Climate Change Between Australia and Antarctica** *Neville Exon, James P. Kennett, and Mitchell Malone (Eds.)*

152 **Sea Salt Aerosol Production: Mechanisms, Methods, Measurements, and Models** *Ernie R. Lewis and Stephen E. Schwartz*

153 **Ecosystems and Land Use Change** *Ruth S. DeFries, Gregory P. Anser, and Richard A. Houghton (Eds.)*

154 **The Rocky Mountain Region—An Evolving Lithosphere: Tectonics, Geochemistry, and Geophysics** *Karl E. Karlstrom and G. Randy Keller (Eds.)*

155 **The Inner Magnetosphere: Physics and Modeling** *Tuija I. Pulkkinen, Nikolai A. Tsyganenko, and Reiner H. W. Friedel (Eds.)*

156 **Particle Acceleration in Astrophysical Plasmas: Geospace and Beyond** *Dennis Gallagher, James Horwitz, Joseph Perez, Robert Preece, and John Quenby (Eds.)*

157 **Seismic Earth: Array Analysis of Broadband Seismograms** *Alan Levander and Guust Nolet (Eds.)*

158 **The Nordic Seas: An Integrated Perspective** *Helge Drange, Trond Dokken, Tore Furevik, Rüdiger Gerdes, and Wolfgang Berger (Eds.)*

159 **Inner Magnetosphere Interactions: New Perspectives From Imaging** *James Burch, Michael Schulz, and Harlan Spence (Eds.)*

160 **Earth's Deep Mantle: Structure, Composition, and Evolution** *Robert D. van der Hilst, Jay D. Bass, Jan Matas, and Jeannot Trampert (Eds.)*

161 **Circulation in the Gulf of Mexico: Observations and Models** *Wilton Sturges and Alexis Lugo-Fernandez (Eds.)*

162 **Dynamics of Fluids and Transport Through Fractured Rock** *Boris Faybishenko, Paul A. Witherspoon, and John Gale (Eds.)*

163 **Remote Sensing of Northern Hydrology: Measuring Environmental Change** *Claude R. Duguay and Alain Pietroniro (Eds.)*

164 **Archean Geodynamics and Environments** *Keith Benn, Jean-Claude Mareschal, and Kent C. Condie (Eds.)*

165 **Solar Eruptions and Energetic Particles** *Natchimuthukonar Gopalswamy, Richard Mewaldt, and Jarmo Torsti (Eds.)*

166 **Back-Arc Spreading Systems: Geological, Biological, Chemical, and Physical Interactions** *David M. Christie, Charles Fisher, Sang-Mook Lee, and Sharon Givens (Eds.)*

167 **Recurrent Magnetic Storms: Corotating Solar Wind Streams** *Bruce Tsurutani, Robert McPherron, Walter Gonzalez, Gang Lu, José H. A. Sobral, and Natchimuthukonar Gopalswamy (Eds.)*

168 **Earth's Deep Water Cycle** *Steven D. Jacobsen and Suzan van der Lee (Eds.)*

169 **Magnetospheric ULF Waves: Synthesis and New Directions** *Kazue Takahashi, Peter J. Chi, Richard E. Denton, and Robert L. Lysal (Eds.)*

170 **Earthquakes: Radiated Energy and the Physics of Faulting** *Rachel Abercrombie, Art McGarr, Hiroo Kanamori, and Giulio Di Toro (Eds.)*

171 **Subsurface Hydrology: Data Integration for Properties and Processes** *David W. Hyndman, Frederick D. Day-Lewis, and Kamini Singha (Eds.)*

172 **Volcanism and Subduction: The Kamchatka Region** *John Eichelberger, Evgenii Gordeev, Minoru Kasahara, Pavel Izbekov, and Johnathan Lees (Eds.)*

173 **Ocean Circulation: Mechanisms and Impacts—Past and Future Changes of Meridional Overturning** *Andreas Schmittner, John C. H. Chiang, and Sidney R. Hemming (Eds.)*

174 **Post-Perovskite: The Last Mantle Phase Transition** *Kei Hirose, John Brodholt, Thorne Lay, and David Yuen (Eds.)*

175 **A Continental Plate Boundary: Tectonics at South Island, New Zealand** *David Okaya, Tim Stern, and Fred Davey (Eds.)*

176 **Exploring Venus as a Terrestrial Planet** *Larry W. Esposito, Ellen R. Stofan, and Thomas E. Cravens (Eds.)*

Geophysical Monograph 177

Ocean Modeling in an Eddying Regime

Matthew W. Hecht
Hiroyasu Hasumi
Editors

American Geophysical Union
Washington, DC

Published under the aegis of the AGU Books Board

Darrell Strobel, Chair; Gray E. Bebout, Joseph E. Borovsky, Kenneth H. Brink, Ralf R. Haese, Robert B. Jackson, W. Berry Lyons, Kenneth R. Minschwaner, Thomas Nicholson, Andrew Nyblade, Nancy N. Rabalais, A. Surjalal Sharma, Chunzai Wang, and Paul David Williams, members.

Library of Congress Cataloging-in-Publication Data

Ocean modeling in an eddying regime / Matthew W. Hecht, Hiroyasu Hasumi, editors.
p. cm. — (Geophysical monograph; 177)
Includes bibliographical references and index.
ISBN 978-0-87590-442-9
1. Oceanography—Mathematical models. 2. Ocean circulation—Mathematical models.
GC10.4.M36026 2008
551.4601′5118—dc22

ISBN: 978-0-87590-442-9
ISSN: 0065-8448

Cover image: Sea surface temperature from a 1/10º global ocean simulation using the LANL Parallel Ocean Program (POP) (courtesy of Mathew E. Maltrud).

2000 Florida Avenue, N.W.
Washington, DC 20009

CONTENTS

Section 3: Modeling at the Mesoscale *State of the Art and Future Directions*

PREFACE

Only a few years after the advent of primitive equation ocean modeling, a new understanding of the importance of oceanic variability began to emerge from observational analysis. The concept of ocean circulation dominated by steady mean currents gave way to a more complex picture in which the prominence and influence of temporal variability were recognized. Accordingly, even in its first decade, ocean modeling began to address the role of eddy variability. Our physical understanding of the influence of variability on the large-scale mean circulation has been built on observations, theory, and modeling.

Earlier ocean modeling of eddying regimes was necessarily performed within idealized models. With advances in computing power and technique, realistic simulation with primitive equation ocean models became possible. Regional simulations with ocean models generating a level of mesoscale variability comparable to that seen from satellite-based altimetry were first completed about a decade ago.

When we refer to a modeled ocean circulation as "strongly eddying," we mean that the spectrum of variability is comparable to that observed at the so-called mesoscale, as defined by the first internal Rossby radius of deformation. In the language of the trade, this is sometimes referred to as eddy-resolving ocean modeling, even if it is only "resolved" in this limited sense.

This monograph is the first to survey progress during this period of realistic simulation in a strongly eddying regime.

The volume opens with an introduction by Frank Bryan, that touches on the content of each of the 20 papers that follow. The rest of the volume is organized into three sections. The first section contains papers that attempt to explain the physical processes involving eddies. These papers can perhaps be thought of as the most recent efforts in a fruitful and long-running pursuit that can be traced back to the early intersection of ocean modeling and the observation of oceanic variability.

The second section addresses realistic modeling of ocean basins. Comparisons with observations are particularly critical here, so the section opens with a paper addressing the subject of appropriate metrics. The section closes with some of the first results from a coupled climate model with an eddying ocean.

The third and final section of the monograph identifies the fronts upon which we anticipate important progress in our field, as seen from our present vantage point. Future advances will bring existing assumptions into question, and so the section opens with a reconsideration of the equations of ocean models.

The editors would like to take this opportunity to acknowledge a number of people whose contributions are greatly appreciated. The staff at AGU Books, including in particular Dawn Seigler, Maxine Aldred, and Carole Saylor, has been most helpful. We would not have attempted this project without the encouragement of Allan Graubard, who was Acquisitions Editor when this monograph was first proposed, before Jeffrey Robbins took over from Allan. Chunzai Wang served as our Oversight Editor. We thank Morrison Bennett, as well as the staff of AGU Books, for the copy editing.

All the papers in this monograph received full peer review, and we thank our many reviewers for their essential contributions.

M.H. gratefully acknowledges the support of the Climate Change Prediction Program within the U.S. Department of Energy's Office of Science. I also acknowledge Bill Holland and Bob Malone, who not only assembled fine programs in ocean modeling, but figure among my most valued mentors.

H.H. acknowledges the late Nobuo Suginohara not only for his personal encouragement to me, but also for his invaluable contribution to Japan's ocean sciences.

Finally, we wish to acknowledge the debt we owe to our late colleague, Peter Killworth, who died on January 28, 2008, of motor neuron disease. Peter influenced ocean modeling and physical oceanography most deeply, and that influence extended to our topic of ocean modeling (or modelling, as Peter would quite sensibly insist) in an eddying regime. From the success of the early Fine Resolution Antarctic Model to the ongoing and ambitious effort to develop a nonhydrostatic finite element based ocean model, Peter made essential contributions to our field. The editors join with all of the authors in dedicating this work to the memory of Peter Killworth.

Matthew W. Hecht
Hiroyasu Hasumi

Ocean Modeling in an Eddying Regime
Geophysical Monograph Series 177

10.1029/177GM01

Introduction: Ocean Modeling—Eddy or Not

Frank O. Bryan

National Center for Atmospheric Research, Boulder, Colorado, USA

Mesoscale eddies are a ubiquitous feature of the ocean circulation, yet are absent from the ocean components of nearly every contemporary climate system model. Progress in ocean modeling over the last decade and advances in high performance computing will soon remedy this dichotomy. Eddy-resolving ocean models are bringing new insights into the physical processes operating in the ocean and will soon find applications in Earth system modeling and weather forecasting. The chapters in this volume provide surveys of the formulation of these models, their ability to simulate the present state of the ocean, and the challenges that remain in refining their accuracy and precision.

1. INTRODUCTION

The atmospheric components of Earth System models simulate climate by explicitly predicting, then averaging over, the day-to-day weather for periods of years to centuries. The weather systems, arising spontaneously as instabilities of the flow established by the equator to pole gradients in solar heating, have spatial scales of O(1,000 km) and time scales of a few days to a week. The weather systems are more than simply noise on the climate state: Their transports of energy, water, and angular momentum are fundamental in establishing the character of the atmospheric circulation and Earth's climate [*Peixoto and Oort*, 1992]. The ocean has weather systems, i.e., mesoscale eddies, dynamically analogous to those in the atmosphere. The majority of the kinetic energy in the ocean is contained in mesoscale eddies and, as in the atmosphere, they are a central part of the dynamical balances of major current systems and in the transport of energy and material through the ocean [*McWilliams*, this volume]. Yet, out of 24 coupled climate models presented in the recent Fourth Assessment Report of the IPCC [*Solomon et al.*, 2007], only one [*K-1 Model Developers*, 2004] attempts to explicitly simulate them. Instead, the flow in nearly every contemporary ocean climate model is represented as essentially laminar, and the effects of ocean mesoscale eddies are entirely parameterized.

Why does this fundamental difference in the approach to modeling atmospheric and oceanic climate dynamics exist? The answer is primarily one of computational economics. Ocean mesoscale eddies have characteristic length scales of O(100 km) or less. With a factor of ten additional grid points required in each horizontal direction and a corresponding decrease in the time step, approximately 1,000 times more computational degrees of freedom are required for an eddy-resolving ocean model compared to an atmosphere model to simulate the global domain for the same period. This computational cost has been impractically high for climate length integrations. With the impending availability of petascale class supercomputers, we will witness a transition in this state of affairs. Fully coupled climate simulations with ocean component models having a resolution of 10 km or better can be expected in the next couple of years. The papers in this volume document the formulation of ocean models of this class, their ability to simulate the various current systems and processes operating in the world ocean, and the challenges that remain in the representation of processes at yet smaller ranges of scales.

Ocean Modeling in an Eddying Regime
Geophysical Monograph Series 177

10.1029/177GM02

2. CURRENT CAPABILITIES

The recognition that ocean mesoscale eddies are a ubiquitous feature of the ocean general circulation led to several

international research programs during the 1970s and early 1980s to investigate their structure and dynamics [*Robinson*, 1983]. The eddy mixing parameterizations used in ocean climate models today are largely based on the theory and understanding developed from those observational programs and the accompanying process modeling studies. These early eddy-resolving ocean model experiments were generally carried out in highly idealized basin configurations and most often using the quasi-geostrophic equations. Under this set of approximations, the basic ocean stratification was prescribed rather than predicted [see *Holland*, [1985] for a comprehensive review].

During the era of the World Ocean Circulation Experiment of the late 1980s and 1990s, basin- to global-scale "eddy-permitting" ocean simulations based on the hydrostatic primitive equations [see *Griffies and Adcroft*, this volume] became computationally practical [*Böning and Semtner*, 2001]. In these models, mesoscale eddies were generally not well resolved spatially, but the explicit dissipation used in the models was reduced to a level where instabilities could at least grow and the flow transitioned from laminar to weakly turbulent. In contrast to the first generation of eddy-resolving models, these simulations included full thermodynamic forcing, and the role of eddies in heat and property transports and water mass formation could begin to be investigated.

Since the turn of the century, we have seen the emergence of basin- to global-scale ocean simulations in which the mesoscale appears to be resolved well enough that global metrics of the simulated mean flow and its variability compare well with available observations [*McClean*, this volume]. The improvements in the simulated circulation have resulted not only from the more accurate representation of mesoscale eddies but also from improvements in the representation of features of the mean flow (such as western boundary currents and their extensions) that have similarly small scales. Perhaps even more fundamentally, the geometry of the ocean domain imposes a tremendous range of scales that can influence the general circulation. Indeed, the first example of a fractal curve described by *Mandlebrot* [1982] is the boundary of the ocean domain—the coastline! Increases in resolution have allowed a more accurate treatment of the basic geometry of the ocean domain, especially narrow straits and passages between basins.

Improvements in the fidelity of the simulated circulation in each of the major ocean basins as model resolution is increased are described in the chapters of this volume. The Southern Ocean is the region where the role of eddies in the fundamental balances of the circulation has been most clearly demonstrated and where the open channel geometry allows the most direct application of theories of eddy–mean flow interaction developed in the atmospheric context [*Ivchenko et al*., this volume; *Tanaka and Hasumi*, this volume]. While state-of-the-art parameterizations of ocean eddies can be tuned to allow coarse resolution models to obtain realistic transports and water mass structures in the Southern Ocean, *Hallberg and Gnanadesikan* [2006] have shown that the transient response to changing forcing (as might occur with a shift in the westerly winds accompanying global warming) is fundamentally different in models with explicitly resolved versus parameterized mesoscale eddies. *Sakamoto and Hasumi* [this volume] show an analogous difference in the response to global warming of the upper ocean circulation in the tropical Pacific for eddy-resolving versus eddy-parameterized models.

One of the most notable systematic biases in coarse-resolution and eddy-permitting ocean models has been a poor simulation of the path of western boundary currents, especially the position of their separation from the coast [*Chassignet and Marshall*, this volume]. As described in the chapters by *Hecht and Smith* [this volume] for the North Atlantic and *Suzuki et al*. [this volume] for the North Pacific, a dramatic improvement in the fidelity of ocean simulations is seen when resolution is increased to around 10 km. The simulations remain quite sensitive to various modeling choices, however, and there remain significant differences between the simulations realized by different models. While eastern boundary regions are less energetic, the important processes setting the basic structure of the flow occur on similarly small scales [*Capet et al.*, this volume].

As mentioned above, the increases in resolution have facilitated not only a better representation of mesoscale eddies but also a more accurate representation of the basic geometry of the ocean domain. *Masumoto et al*. [this volume] provide a prominent example of this for the Indian Ocean where the water mass properties are strongly influenced by flow through a series of narrow passages in the Indonesian Throughflow. The simulation of exchanges between the subpolar regions and the Arctic has also been shown to be significantly improved with increases in resolution to below 10 km [*Maslowski et al*., this volume], with important implications for the heat budget and ice distributions in that basin.

3. FUTURE DIRECTIONS

The improvements in the fidelity of ocean models achieved over the last several years represent a significant milestone in ocean research but should, by no means, be considered an end point. Global coupled climate simulations have just recently entered the "eddy-permitting" regime, and eddy-resolving stand-alone ocean simulations have been integrated for less than a century [*Masumoto et al*., 2004]. The next several years should see a broader application of eddy-resolving models

not just in studies of ocean dynamics but also in the broader context of Earth system modeling including biogeochemical processes [*Oschlies*, this volume] and operational environmental forecasting systems [*Hurlburt et al.*, this volume].

There is no indication that the "eddy-resolving" solutions obtained to date have converged even for quasi-geostrophic dynamics [*Siegel et al*., 2001], and the current generation of models remain quite sensitive to any number of choices in model configuration and sub-grid-scale closure [*Hecht et al*., this volume]. That is, we are still far from "large eddy simulation" for global ocean models. It is inevitable that models with increasingly finer resolution will be constructed, although potentially more resource-efficient methods such as nested grids [*Capet et al*., this volume] or adaptive grid methods [*Piggott et al*., this volume] may see increased application.

Moving into the eddying regime presents new challenges and opportunities in developing parameterizations of processes occurring at yet smaller scales. *Fox-Kemper and Menemenlis* [this volume] and *Hecht et al*. [this volume] describe several approaches for subgrid-scale closures more appropriate for the situation where the turbulent cascade is partially resolved. The expanded range of explicitly resolved scales opens the opportunity for putting parameterizations of processes such as inertial wave excitation and propagation [*Klein*, this volume], gravity currents [*Legg et al*., this volume], and mixed-layer restratification [*Thomas et al*., this volume] on a firmer physical foundation.

Acknowledgments. NCAR is supported by the National Science Foundation.

REFERENCES

Böning, C. W., and A. J. Semtner (2001), High-resolution modeling of the thermohaline and wind-driven circulation, in *Ocean Circulation and Climate*, edited by G. Siedler, J. Church, and J. Gould, pp. 59–71, Academic, New York.

Hallberg, R., and A. Gnanadesikan (2006), The role of eddies in determining the structure and response of the wind-driven Southern Hemisphere overturning: Results from the Modeling Eddies in the Southern Ocean (MESO) Project, *J. Phys. Oceanogr*., *36*, 2232–2252.

Holland, W. R. (1985), Simulation of mesoscale variability in midlatitude gyres, in: *Issues in Atmospheric and Oceanic Modeling. Part A: Climate Dynamics*, edited by S. Manabe, pp. 479–523, Academic, New York.

K-1 Model Developers (2004), K-1 Coupled GCM (MIROC) Description. Center for Climate System Research, University of Tokyo. Available at: www.ccsr.u-tokyo.ac.jp/kyosei/hasumi/MIROC/tech-repo.pdf.

Mandelbrot, B. (1982), *The Fractal Geometry of Nature,* 420 pp., W.H. Freeman, New York.

Masumoto, Y., H. Sasaki, T. Kagimoto, N. Komori, A. Ishida, Y. Sasai, T. Miyama, T. Motoi, H. Mitsudera, K. Takhashi, H. Sakuma, and T. Yamagata (2004), A fifty-year simulation of the world ocean—Preliminary outcomes of OFES (OGCM for the Earth Simulator), *J. Earth Simulator*, *1*, 35–56.

Peixoto, J. P., and A. H. Oort (1992), *Physics of Climate*, 520 pp., American Institute of Physics, New York.

Robinson, A. R. (1983), *Eddies in Marine Science*, 609 pp., Springer, Berlin.

Siegel, A., J. B. Weiss, J. Toomre, J. C. McWilliams, P. S. Berloff, and I. Yavneh (2001), Eddies and vortices in ocean basin dynamics, *Geophys. Res. Lett*., *28*, 3183–3186.

Solomon, S., D. Qin, M. Manning, Z. Chen, M. Marquis, K. B. Averyt, M. Tignor, and H. L. Miller (2007), *Climate Change 2007: The Physical Science Basis. Contribution of Working Group I to the Fourth Assessment Report of the Intergovernmental Panel on Climate Change,* 996 pp., Cambridge University Press, Cambridge.

Frank Bryan, Climate and Global Dynamics Division, National Center for Atmospheric Research, Boulder, CO 80307, USA.

The Nature and Consequences of Oceanic Eddies

James C. McWilliams

Department of Atmospheric and Oceanic Sciences, University of California, Los Angeles, California, USA

Mesoscale eddies are everywhere in the ocean. They provide important material and dynamical fluxes for the equilibrium balances of the general circulation and climate. Eddy effects are necessary ingredients for oceanic general circulation models, whether parameterized or, as is increasingly done, explicitly resolved in the simulations. The primary characteristics of eddies are summarized in this paper, and the principal roles of eddies in the dynamics of large-scale circulation are described. Those eddy roles are the following: maintenance of boundary and equatorial currents; lateral and vertical buoyancy fluxes, isopycnal form stress, and available potential energy conversion; Reynolds stress, kinetic energy conversion, and current rectification; material dispersion and mixing; energy cascades and dissipation routes; Lagrangian mean advection; surface-layer density restratification; ventilation and subduction; stratification control; frontogenesis; topographic form stress; biological pumping and quenching; and generation of intrinsic climate variability.

1. INTRODUCTION

Mesoscale eddies pervade the ocean (e.g., Plates 1 and 2 and *Stammer* [1997]), and they usually account for the peak in the kinetic energy spectrum [*Wunsch and Stammer*, 1995]. For the most part, they arise from instabilities of more directly forced, persistent currents. Consequently, they play a central role in limiting the strength of the persistent currents. How eddies play this role can be expressed qualitatively as an effective eddy viscosity that spreads and dissipates the parent currents (although the language of eddy diffusion is notoriously subtle in fluid dynamics). Similarly, eddies disperse material concentrations, largely along isentropic/isopycnal surfaces in the stratified interior, and this role can be expressed as an anisotropic eddy diffusion[1] as well as, somewhat more subtly, an eddy-induced advection. Of course, in the nonstationary, inhomogeneous four-dimensional structure of the oceanic general circulation and climate, such simple characterizations of the effects of eddies—i.e., the eddy-averaged fluxes due to eddy-fluctuation covariances—are far from the whole story. This essay surveys the conceptual landscape of eddy effects at a qualitative level. It does not delve deeply into how these effects are, or should be, represented in models either by parameterizations or direct simulation. These subjects are large ones, while the essay is relatively short and much less than a comprehensive review.

Oceanic spectra are broad band. The mesoscale range is centered around horizontal scales L of tens and hundreds of kilometers. L is close to the first baroclinic deformation radius, $R_d \approx NH/f$ outside the tropics or $R_d \approx \sqrt{NH/\beta}$ near the equator [*Stammer*, 1997]. N is the buoyancy frequency in the main pycnocline, H its depth, f the Coriolis frequency, and β the meridional gradient of f. R_d is much smaller than most basin widths. The most energetic vertical scales are relatively large, comparable to H or the oceanic depth D. The evolutionary timescales range from $(\beta L)^{-1}$ ~ days—for larger scale barotopic Rossby waves with $L > R_d$—to $R_d V^{-1}$ (V is the horizontal velocity) or $(\beta R_d)^{-1}$ ~ weeks and months—for baroclinic eddies [*Chelton et al*., 2007]—and even to years—for some coherent vortices like Meddies [*McWilliams*, 1985] that survive until some destructive encounter with another

Ocean Modeling in an Eddying Regime
Geophysical Monograph Series 177

10.1029/177GM03

strong current or steep topography. The spatial distribution of eddy energy is quite inhomogeneous with the highest energy near the major persistent currents, e.g., the Gulf Stream and Antarctic Circumpolar Current [*Ducet et al*., 2000].

For present purposes, it is useful to decompose oceanic currents and material concentration variations into four components: large-scale, mesoscale, submesoscale, and microscale. Climate and general circulation models simulate the large-scale distributions, with mesoscale eddy effects either parameterized or at least partially resolved (following the strategy of large eddy simulation; *Pope* [2000]). We must acknowledge, however, that we are still several computer generations away from being able to fully and routinely resolve the mesoscale in global climate models (e.g., with a horizontal grid scale of 5 km and a model integration time of centuries).

Submesoscale eddies are defined as smaller than the mesoscale while still significantly influenced by Earth's rotation and density stratification. They are not resolved in modern oceanic general circulation models (OGCMs). Determining which submesoscale effects need to be parameterized in OGCMs is still very much a future frontier. Among the most plausibly important effects are density restratification, especially in the surface layer [*Rudnick and Ferrari*, 1999], and a route to energy dissipation for the mesoscale [*Muller et al.*, 2005]. Parameterization of microscale effects are important for the turbulent boundary layers at the top, bottom, and sides (if any) and for the interior diapycnal mixing of materials across stably stratified isopycnal surfaces.

These are interesting times in the science of eddies and the general circulation. The theoretical framework for eddy dynamics is well established, as are the observational and modeling bases for eddy structure and phenomenology. But the observational basis for eddy fluxes is still quite sparse, and no measurement techniques in prospect are likely to change this greatly. There is a modeling path for establishing "eddy-flux truth," but this path probably requires much higher resolutions than are commonly used as yet, and probably further refinements in submesoscale and microscale parameterizations are necessary as well to become demonstrably robust and reproducible. The papers in this book comprise a status report on eddy-resolving ocean modeling.

2. EDDY THEORY AND MODELING

Mesoscale eddy flows are understood by oceanographers to satisfy approximately the diagnostic force balances, viz., geostrophic in the horizontal and hydrostatic in the vertical. This is a consequence of their dynamical parameter regime with small Rossby number, Froude number, and aspect ratio:

$$Ro = \frac{V}{fL}, Fr = \frac{V}{NH}, \lambda = \frac{H}{L} \ll 1 . \tag{1}$$

In this regime, the asymptotic dynamical model is quasi-geostrophy:

$$[\partial_t + \mathbf{v}_g \cdot \nabla_h] q_{qg} = NCE , \tag{2}$$

where

$$\begin{aligned} q_{qg} &= f_0 + \beta(y - y_0) + \frac{1}{f_0}\nabla_h^2 \phi + f_0 \partial_z \left(\frac{b}{N^2(z)} \right) \\ &\quad - \frac{f_0(D - D_0)}{H_b}\delta[z, -D_0] + \frac{f_0 b}{H_s N^2}\delta[z, 0] , \\ \mathbf{v}_h &\approx \mathbf{v}_g = f_0^{-1}\hat{\mathbf{z}} \times \nabla_h \phi , \\ b &= \partial_z \phi \approx g\left(\tilde{\alpha}_0(T - T_0) - \tilde{\beta}_0(S - S_0) \right) . \end{aligned} \tag{3}$$

The subscript 0 denotes a constant reference value. The subscript h denotes the horizontal component of a vector, and x and y are the zonal (eastward) and meridional (northward) horizontal coordinates. The upward vertical coordinate is z; $\hat{\mathbf{z}}$ is its unit vector; $z = 0$ is mean sea level; and $z = -D(\mathbf{x}_h)$ is the bottom. $\mathbf{v}_g$ is geostrophic velocity; ϕ is geopotential function (dynamic pressure); b is buoyancy variation around the mean stratification, $\int N^2(z)dz$; T is temperature; and S is salinity. g is gravitational acceleration; $\tilde{\alpha}$ and $\tilde{\beta}$ are thermal-expansion and haline-contraction coefficients; and q_{qg} is quasi-geostrophic potential vorticity. NCE indicates nonconservative effects associated with submesoscale and microscale stirring and mixing parameterizations, which usually have small rates except near the surface and bottom where they convey boundary stress and material fluxes into the ocean. H_s and H_b are constant vertical layer thicknesses adjacent to the surface and bottom, and $\delta[a,b]$ is a discrete delta function equal to one when $a = b$ and zero otherwise.

Almost all our understanding of eddy dynamics and phenomena has its roots in quasi-geostrophic theory and its extensive body of analytical and computational solutions [*Pedlosky*, 1987; *McWilliams*, 2006; *Vallis*, 2006]. This provides paradigms for

- –*wave and vortex propagation* due to β and due to horizontal gradients of topography $\nabla_h D$ and other persistent components of potential vorticity $\nabla_h \langle q \rangle$ (brackets denote an average over eddies);
- –long-lived *coherent vortices* at both the mesoscale and smaller;

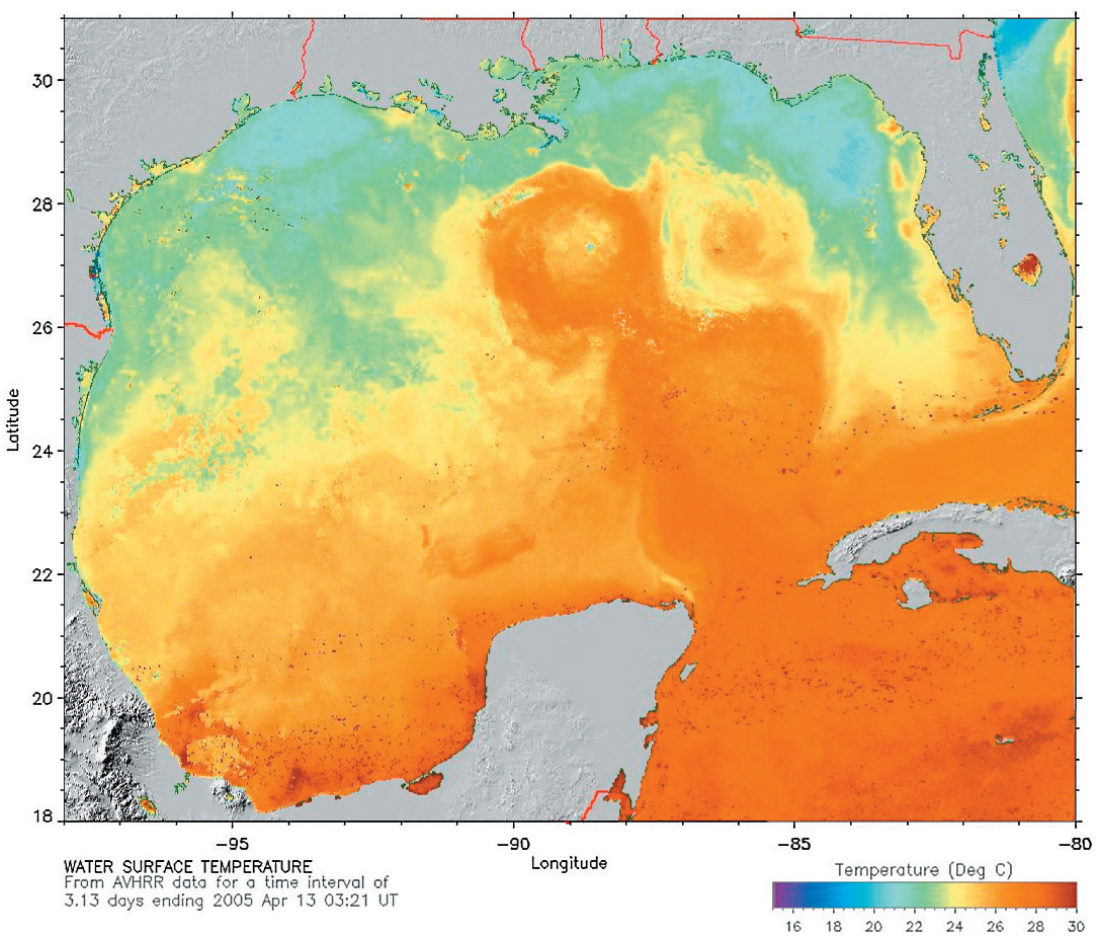

Plate 1. Anticyclonic eddies in the Gulf of Mexico detaching from the Loop Current sector of the Gulf Stream between the Yucatan and Florida Straits in April 2005. Eddy generation occurs quasi-annually and typically is followed by westward propagation across the basin [*Hurlburt and Thomson*, 1980; *Sturgis and Leben*, 2000]. Their diameters are approximately 250 km (courtesy of the Ocean Remote Sensing Group, Johns Hopkins University Applied Physics Laboratory).

Plate 2. Oceanic eddies in Davis Strait (north of the Labrador Sea, west of Greenland) during June 2002. The eddies are made visible by sea-ice fragments. The eddies arise as an instability of the boundary current along the ice margin. Their diameters are approximately 25 km (courtesy of Jacques Descloirest, NASA Goddard Space Flight Center).

–*geostrophic turbulence* with its forward cascade (i.e., transfer of variance across spatial scales) of $\langle q_{qg}^2 \rangle$ and inverse cascade of energy;
–*eddy generation* by baroclinic and barotropic instabilities feeding off of $\partial_z \langle \mathbf{v}_g \rangle$ and $\nabla_h \langle \mathbf{v}_g \rangle$, respectively;
–*eddy fluxes* in idealized zonal jets and wind gyres, with eddy potential vorticity flux, $\langle \mathbf{v}_g' q_{qg}' \rangle$, playing a central dynamical role due to the advective conservation form of (2) and the nondivergence of $\mathbf{v}_g'$ (n.b., the eddy q flux combines the separate individual Reynolds stress, form stresses, and buoyancy fluxes discussed in section 3);
–*topology* of potential vorticity on horizontal or isopycnal surfaces, both as barriers or conduits for transport (i.e., boundary-intersecting, open contours or contours closed within the flow domain) and as undergoing time-reversible or irreversible deformations (i.e., waves or turbulence); and
–*surface frontogenesis* involving $\nabla_h b(x,y,0,t)$ in the final q_{qg} term in (3).

The quasi-geostrophic equations (2) and (3) are essentially a local model on the eddy scale (i.e., $L \approx R_d$). They lose accuracy and relevance on the larger scales of the general circulation as well as on finer submesoscales and microscales. For this reason and for the purpose of geographically realistic simulations, the usual practice is to base an OGCM on the hydrostatic primitive equations (i.e., not assuming small Ro, Fr, β_0/f_0, and $|D - D_0| / D_0$); on the full equation of state for seawater; and on realistic surface forcing and topography [*McWilliams*, 1996]. This imposes a gap between idealized eddy theory and realistic OGCM simulation. The gap is widened by the computational compromises required for general circulation and climate simulations. Nevertheless, the past decade has seen a rapid increase in eddy-resolving OGCM simulations, as increased computational capacity has made them at least somewhat feasible. No doubt, the future will be dominated by fully eddy-resolving OGCMs, while the present time is a transitional stage when many lessons are still being learned about how they should be configured.

3. EDDY ROLES IN CIRCULATION AND CLIMATE

In an OGCM, the large-scale circulation is explicitly calculated. The dynamical effects of mesoscale eddies must then be either parameterized or explicitly calculated. In either case, it is necessary to understand what the important eddy effects are. This problem is a particular example of the eddy-mean interactions that are so central to fluid dynamics. Here, the mean is identified with the large-scale flow and material distributions. This section surveys the principal eddy effects as presently understood. In most aspects, the quantitative measures of these effects in nature and in OGCMs are still at a rather rudimentary level, and future work will have to improve the tests and probably modify our understanding of the eddy roles.

We continue to use angle brackets to denote an average over the eddies (i.e., the mean) and use a prime to denote a band-pass filter applied to the residual fluctuations centered on the mesoscales (i.e., the eddies). The eddy effects are expressed through eddy flux divergences that contribute to the mean tendency of any advected quantity A:

$$\frac{\partial \langle A \rangle}{\partial t} + \ldots = -\nabla \cdot \langle \mathbf{v}' A' \rangle \,, \tag{4}$$

where the dots are a placeholder for the other evolutionary influences on $\langle A \rangle$, and $\mathbf{v}$ is assumed to be nondivergent. In oceanic models, A is relevant to momentum $\mathbf{v}$, vorticity, buoyancy b, potential vorticity q, and many material properties (e.g., temperature T, salinity S, biological nutrients, and organisms). Eddy effects on other quantities of interest, such as energy and its dissipation rate, are assessed by derivations from the primary governing equations in the form of (4).

3.1. Eddy Maintenance of Boundary and Equatorial Currents

Since the work of *Munk* [1950], it has been understood that the western boundary currents in extra-tropical wind gyres are dynamically supported by eddies in a way that could be parameterized with a horizontal eddy viscosity ν_h. All OGCMs have some form of ν_h, and the associated boundary layer thickness, $L_\nu \sim \nu_h/\beta)^{1/3}$, must be at least as large as a few grid cells to support a lateral boundary stress (and perhaps also suppress computational noise). Simulations with well-resolved boundary currents and a small ν_h value relegate the direct influence of ν_h to within the near-boundary region, while explicit eddy instabilities give rise to momentum flux $\langle \mathbf{v}'\mathbf{v}' \rangle$ (Reynolds stress) and buoyancy flux $\langle \mathbf{v}' b' \rangle$ that further act to maintain and reshape the mean currents, not always in ways consistent with Munk's simple modeling concept (cf. sections 3.2 and 3.6). In the broad sweep of oceanic theory and modeling, horizontal and vertical eddy viscosities have often been invoked for the maintenance of mean currents near boundaries and the equator as a means of balancing their persistent forcing. This perspective seems less apt for the Antarctic Circumpolar Current and the eastward extension of separated western boundary currents where the important eddy effects are better characterized in ways other than by an eddy viscosity based on a down-gradient Reynolds stress.

3.2. Eddy Buoyancy Flux, Isopycnal Form Stress, and Potential Energy Conversion

In the mean circulation, the potential energy—or, more precisely, the available potential energy $\sim\int \langle b\rangle^2/\ 2N^2 d\mathbf{x}$—dominates the kinetic energy $\int \langle \mathbf{v}\rangle^2/\ 2 d\mathbf{x}$, roughly by the ratio $(L_m/L_d)^2 \gg 1$ (L_m is the horizontal scale of the mean flow; *Gill et al.* [1974]). An effective route for energy dissipation of the mean circulation is by conversion of mean potential energy into eddy energy with $\int \langle w'b'\rangle d\mathbf{x} > 0$ (w is vertical velocity). This is often associated with baroclinic instability where fluctuations amplify with an associated horizontal buoyancy flux $\langle \mathbf{v}_h' b'\rangle$ that is negatively correlated with the mean buoyancy gradient $\nabla_h\langle b\rangle$ (cf., section 3.5). With geostrophic balance, this also implies a correlation with the mean vertical shear $\partial_z\langle \mathbf{v}_h\rangle$. This has the effect of vertical momentum transfer, hence reduction of mean shear, through an eddy form stress $f_0\hat{\mathbf{z}}\times\langle \mathbf{v}_h'\eta'\rangle$ acting on approximately impenetrable density surfaces in the stably stratified interior region ($\eta \approx -b/N^2$ is the vertical displacement of an isopycnal surface from its resting level). As a parameterization representation, these effects can be expressed as lateral eddy diffusion of buoyancy with diffusivity κ_h—and, even better, as lateral diffusion of the "thickness" between isopycnal surfaces, $\partial\langle\eta\rangle/\partial b$, which has a quasi-adiabatic effect on the mean buoyancy field [*Gent and McWilliams*, 1990]—or vertical eddy viscosity for horizontal velocity, with an equivalent eddy viscosity, $\nu_v \approx \kappa_h\ (f/N)^2$. This process for eddy equilibration and dissipation of the mean circulation is particularly apt for the Antarctic Circumpolar Current [*Marshall*, 1981; *McWilliams and Chow*, 1981; *Gent et al*., 1995], and it is also quite widespread, as most large-scale currents are concentrated in the upper ocean and thus have substantial vertical shear. Baroclinic energy conversion is probably the dominant route to dissipation from the general circulation through the mesoscale [*Wunsch and Ferrari*, 2004], although microscale boundary-layer turbulence also contributes significantly (section 3.4).

3.3. Eddy Dispersion and Mixing

As usual, in turbulent flows, the Lagrangian autocorrelation time is finite for mesoscale eddy trajectories, and particle dispersion,

$$D(t) = \langle \mathbf{X}'^2\rangle,$$

is a monotonically increasing function over intervals of days to months ($\mathbf{X}'(t) = \int \mathbf{v}' dt$ is the Lagrangian position following the eddy velocity). These behaviors support the interpretation of eddy mixing for material concentrations and, more heuristically, since the pressure force breaks Lagrangian conservation, for momentum as well. The associated Lagrangian diffusivity, $\kappa = d_t D$, is usually found to be consistent with a "mixing-length" estimate, $\kappa \sim V' L_d = O(10^3)\ \mathrm{m^2\ s^{-1}}$, based on mesoscale currents [*Krauss and Böning*, 1987; *Sundermeyer and Price*, 1998]. Such a diffusivity magnitude has a significant dispersal effect across oceanic gyres over a period of decades. In quasi-geostrophic theory (section 2), eddy trajectories are entirely horizontal following the geostrophic flow, and it is physically plausible that this constraint can be generalized to their confinement to isopycnal surfaces with small slopes in the stably stratified, nearly adiabatic oceanic interior. Thus, eddy dispersion and mixing are highly anisotropic, acting much more in isopycnal directions than diapycnal.[2] This leads to a degree of homogenization for passively advected material concentrations within closed geostrophic circulation contours on isopycnal surfaces (as has long been noted by hydrographers), limited by the geographical distribution of their diabatic sources and sinks. As potential vorticity q is also conserved on trajectories except for mixing effects, it too may become homogenized through eddy isopycnal mixing within mean recirculation gyres under some conditions [*Rhines and Young*, 1982]. This is potentially a strong dynamical constraint on the 3D structure of the mean circulation [e.g., as in the inversion of q_{qg} for φ and $\mathbf{v}_g$ in (3)]; however, the present evidence in favor of potential-vorticity homogenization is more evident in quasi-geostrophic models than in OGCMs.

3.4. Eddy Energy Cascades

Once energy is transferred from the general circulation into the eddy field, eddy advective dynamics lead to transfers of variance across spatial scales, commonly referred to as a cascade. The paradigm for eddy cascades is geostrophic turbulence theory [*Charney*, 1971]. The theory predicts that eddy energy has an inverse cascade toward larger scales both vertically and horizontally; that there is an approximately equipartition between kinetic and available potential energy; that potential enstrophy $\langle q_{qg}'^2\rangle$ cascades toward smaller scales (hence to its dissipation); and that dynamically passive material tracers cascade toward smaller horizontal scale without any vertical exchanges. These predictions are for a vertically unbounded domain. With a finite depth, the baroclinic eddies with $L \gg L_d$ cascade into barotopic eddies with L near L_{d} and thereafter exhibit an inverse cascade in horizontal scale [*Salmon*, 1982; *Larichev and Held*, 1995]. These cascades can be impeded by large-scale potential vorticity gradients associated with f, D, or $\langle \mathbf{v}_h\rangle$, e.g., for the Coriolis frequency,

the arrest scale is $L_\beta = (V'/\beta)'^{1/2}$ [*Rhines*, 1975], with typical values of hundreds of kilometers in the ocean (i.e., larger than L_d). Barotropic currents, in particular, can be dissipated through bottom boundary layer drag, which provides one important route to dissipation for eddy energy. There may also be an important forward eddy energy cascade into the submesoscale in the interior associated with a breakdown of the geostrophic and even more general diagnostic force balances [*Muller et al*., 2005; *Capet et al.*, 2008a; Molemaker et al., Balanced and unbalanced routes to dissipation in an equilibrated Eady flow, submitted to *Journal of Fluid Mechanics*, 2007, hereinafter referred to as Molemaker et al., submitted manuscript, 2007], followed by further forward cascade to the microscale and dissipation scale. *Scott and Wang* [2005] show observational evidence for such a forward cascade at least with respect to eddy kinetic energy. Eddy routes to dissipation are a necessary accompaniment for eddy depletion of the general circulation through mean-current instabilities (sections 3.2 and 3.6).

3.5. Eddy-Induced Lagrangian Transport

Any vector can be decomposed with respect to any other vector. For eddy transport, it is relevant to decompose eddy buoyancy flux $\langle \mathbf{v}'b' \rangle$ relative to the mean buoyancy gradient $\nabla\langle b \rangle$:

$$\langle \mathbf{v}'b' \rangle = -\frac{\langle \mathbf{v}'b' \rangle \times \nabla \langle b \rangle}{|\nabla \langle b \rangle|^2} \times \nabla \langle b \rangle + \frac{\langle \mathbf{v}'b' \rangle \cdot \nabla \langle b \rangle}{|\nabla \langle b \rangle|^2} \nabla \langle b \rangle$$
$$\equiv \Psi^* \times \nabla \langle b \rangle + \mathbf{R}^*[\langle b \rangle]. \quad (5)$$

The separate terms represent eddy fluxes along and across mean buoyancy surfaces (i.e., isopycnal and diapycnal, with the former component also referred to as the skew flux, perpendicular to the mean buoyancy gradient; *Griffies* [1998]). The final relation in (5) implicitly defines the eddy-induced streamfunction Ψ^* and residual buoyancy flux $\mathbf{R}^*[\langle b \rangle]$. We further define an eddy-induced velocity,

$$\mathbf{v}^* = \nabla \times \Psi^*. \quad (6)$$

We can readily show that $\mathbf{v}^*$ is nondivergent, $\nabla \cdot \mathbf{v}^* = 0$ (as is the Eulerian velocity in an incompressible fluid) and that it provides an eddy-induced buoyancy advection in the mean buoyancy equation,[3]

$$\nabla \cdot \langle \mathbf{v}'b' \rangle = \mathbf{v}^* \cdot \nabla \langle b \rangle + \nabla \cdot \mathbf{R}^*[\langle b \rangle]. \quad (7)$$

This formal decomposition of the eddy buoyancy flux allows a statement of the physical hypothesis that the diapycnal flux $\mathbf{R}^*[\langle b \rangle]$ is very small in the stably stratified, nearly adiabatic interior of the ocean (i.e., outside the turbulent boundary layers) where b is almost conserved along trajectories over several eddy fluctuation cycles [*Gent and McWilliams*, 1990; *Gent et al*., 1995]. This implies that the only important eddy effect on the baroclinic dynamics of the circulation is an additional buoyancy advection by $\mathbf{v}^*$, which can thus be considered part of the Lagrangian mean flow[4] when it is added to $\langle \mathbf{v} \rangle$. When eddies act to extract mean available potential energy (section 3.2), $\mathbf{v}^*$ is an overturning circulation acting to flatten mean isopycnal surfaces. A conspicuous example of this is the meridional overturning cell in the Antarctic Circumpolar Current that is opposite to the Eulerian-mean Deacon Cell (i.e., $\hat{\mathbf{x}} \cdot \Psi^* > 0$ in the center of the current).

The interpretation of eddy-induced advection extends to the eddy flux of any material concentration c with the decomposition,

$$\langle \mathbf{v}'c' \rangle \equiv \Psi^* \times \nabla \langle c \rangle + \mathbf{R}^*[\langle c \rangle]. \quad (8)$$

Again, the eddy-induced Lagrangian velocity $\mathbf{v}^*$, defined in terms of the eddy buoyancy flux, contributes an advective tendency for $\langle c \rangle$, but now, the residual material flux $\mathbf{R}^*[\langle c \rangle]$ includes fluxes both along the mean buoyancy surfaces as well as across them [$\mathbf{R}^*$ here is defined by making a decomposition of $\langle \mathbf{v}'c' \rangle$ perpendicular and parallel to $\langle \nabla \langle c \rangle \rangle$, analogous to (5) relative to $\langle \nabla \langle b \rangle \rangle$, and then by subtracting the first term in (8)]. The isopycnal component is not expected to be small and is often interpreted and modeled as isopycnal eddy diffusion of $\langle c \rangle$ (section 3.3; *Redi* [1982]). The diapycnal component of $\mathbf{R}^*[\langle c \rangle]$ is still expected to be small if eddy trajectories are approximately confined to isopycnal surfaces.

This quasi-adiabatic characterization of eddy fluxes does not hold within the turbulent boundary layers [*Tandon and Garett*, 1996], and the eddy material fluxes in (5) and (8) both develop stronger diapycnal components and rotate toward a boundary-parallel orientation to preclude any boundary-normal flux [*Ferrari et al*., 2008].

3.6. Eddy Reynolds Stress, Kinetic Energy Conversion, and Current Rectification

Barotropic instability allows eddies to grow at the expense of the mean current (section 3.1) when the horizontal Reynolds stress $\langle \mathbf{v}'_h \mathbf{v}'_h \rangle$ has a negative tensor correlation with the mean horizontal shear $\nabla \langle \mathbf{v}_h \rangle$, i.e., it acts in the sense of an eddy flux down the mean gradient, consistent with a positive horizontal eddy viscosity, $\nu_h > 0$, and it effects a conversion from mean to eddy kinetic energy. Vertical Reynolds stress

is much less likely to be significant for eddies because their vertical velocity w' is so weak (section 2). The Loop Current in the Gulf of Mexico exhibits this behavior, with finite fluctuation amplitudes leading to the detachment of large, anticyclonic eddies (Figure 1; *Hurlburt and Thompson* [1980]). There is similar, if limited, evidence for down-gradient momentum flux in the Gulf Stream along the western boundary [*Dewar and Bane*, 1985] in the location where such an effect is expected from gyre theory (section 3.1). However, there is a competing paradigm for $\langle \mathbf{v}'_h \mathbf{v}'_h \rangle$, viz., it can accelerate a mean current by β-induced Rossby wave radiation away from a source region of eddy fluctuations [*Haidvogel and Rhines*, 1983; *Berloff*, 2005]. There is observational evidence for this effect, e.g., near the offshore Kuroshio Current [*Tai and White*, 1990]. In particular, this type of "negative viscosity" ($\nu_h < 0$), eddy-rectification behavior is common for baroclinically unstable (section 3.2), eastward jets [*Marshall*, 1981; *McWilliams and Chow*, 1981]. It is an example of spatially nonlocal eddy-mean interaction where wave propagation establishes a connection between the mean flows in the separated locations of wave generation and dissipation.

3.7. Eddy Restratification

The eddy-induced conversion of mean available potential energy and associated Lagrangian mean circulation (sections 3.2 and 3.5) have the effect of restratifying the ocean by flattening the tilted isopycnal surfaces. This effect is widespread for the tilted pycnocline surfaces associated with baroclinic, geostrophic mean currents. It can have an especially dramatic effect after episodes of deep convective boundary-layer mixing that usually occur with significant lateral inhomogeneity (e.g., in the Labrador and Mediterranean Seas). In this configuration, the isopycnal surfaces surrounding the convection zone are very steeply tilted, and they geostrophically support a strong, vertically sheared rim current. The ensuing baroclinic instability of the rim current leads to efficient lateral and vertical eddy buoyancy fluxes $\langle \mathbf{v}' b' \rangle$ and restratifies the convectively mixed water mass [*Joes and Marshall*, 1997; *Katsman et al*., 2004], typically on timescales of weeks and months. Another situation where this effect is important is in the surface boundary layer when there are horizontal buoyancy gradients $\nabla\langle b \rangle$, weak geostrophic vertical shear, and weak stratification. The resulting baroclinic instability occurs on rather small scales (often more submesoscale than mesoscale), and it acts to restratify the "mixed layer" and thus competes against the microscale turbulent mixing generated by surface wind and buoyancy fluxes [*Boccaletti et al*., 2007; *Capet et al*., 2008a]. This eddy restratification effect may be particularly evident after strong surface fluxes abate.

3.8. Eddy Ventilation and Subduction

Where isopycnal surfaces intersect either the surface or bottom boundaries, a quasi-adiabatic pathway opens into the oceanic interior. This can provide a ventilation of the interior region to anomalous material concentrations generated through microscale boundary-layer mixing [*Armi*, 1978; *Garrett*, 1979] and surface fluxes. While boundary-normal eddy fluxes are zero at the boundaries (section 3.5), they increase into the interior on the scale of the boundary-layer thickness [*Ferrari et al*., 2008]. The situation where surface-layer materials are carried down into the interior is referred to as eddy subduction, and it may be accomplished either by eddy mixing or by eddy-induced advection (sections 3.3 and 3.5) [*Marshall*, 1997; *Hazeleger and Drijfthout, 2000*].

3.9. Eddy-Controlled Stratification

Implicit in the eddy roles in material transport and buoyancy flux (sections 3.2, 3.3, and 3.5) are eddy influences on the 3D distribution of $\langle b \rangle$, including its vertical profile, i.e., the stratification. The idea of eddy control of stratification is explicitly addressed in several idealized models where eddy fluxes establish the pycnocline slope beneath the diabatic surface boundary layer. With the surface horizontal gradient $\nabla_h \langle b \rangle$ strongly constrained by large-scale air-sea interaction (i.e., by atmospheric climatological distributions), the vertical gradient $\partial_z \langle b \rangle$ is determined from $\nabla_h \langle b \rangle$ divided by the pycnocline slope. This characterization is most fully developed for flows without zonal boundaries, hence relevant to the Antarctic Circumpolar Current [*Marshall et al*., 2002; *Marshall and Radko*, 2003; *Cessi and Fantini*, 2004; *Olbers and Visbeck*, 2005] as well as to the tropospheric Westerly Winds.

3.10. Eddy-Induced Frontogenesis

As analyzed by *Hoskins and Bretherton* [1972], a horizontal strain flow induces frontogenesis by sharpening horizontal buoyancy gradients, especially near the surface boundary. In the ocean, this process occurs both due to the large-scale circulation (e.g., the subtropical fronts near the equatorward edge of subtropical wind gyres) and a fortiori due to mesoscale eddies because of their larger strain rates [*Capet et al*., 2008a]. Frontogenesis involves a conversion of available potential energy into kinetic energy (section 3.2) on increasingly smaller horizontal scales reaching into the submesoscale, and the ensuing frontal instabilities can further feed into a forward eddy energy cascade (section 3.4; Molemaker et al., submitted manuscript, 2007). Frontogenesis is an effective means of upper-ocean restratification

(section 3.7), and it contributes to eddy ventilation and subduction partly through secondary circulation in the cross-frontal plane (section 3.8; *Thomas et al*. [2007]). The surface quasi-geostrophic model—i.e., (2) and (3) with q_{qg} including the final term with surface buoyancy variations but having a uniform interior value—depicts the mesoscale frontogenesis process fairly well but excludes some important frontal instability behaviors [*Held et al*., 1995]; it also captures the forward cascade of available potential energy and conversion into kinetic energy that occurs in a turbulent field of surface fronts *Capet et al.* [2008a, 2008b].

3.11. Topographic Form Stress and Rectification

Eddies play at least two important roles in combination with topography in shaping the large-scale circulation. The most direct influence is by providing a drag force at the bottom, viz., the integrated horizontal pressure force against the bottom, the form stress $\langle \phi' \nabla_h D' \rangle$. The form stress be rewritten as $f_0 \hat{\mathbf{z}} \times \langle \mathbf{v}'_g D' \rangle$ with the geostrophic approximation (cf., isopycnal form stress in section 3.2). As D' is steady in time in this context, the relevant eddies are also the steady deviations from the large-scale flow, i.e., the standing eddies. Form stress provides the principal balancing force to the wind stress in the Antarctic Circumpolar Current [*Treguir and McWilliams*, 1990; *Wolff et al*, 1991], and it probably is significant in other places where mean currents extend to the bottom and cross topographic contours. A different type of influence is the effect of transient eddies over a topographic slope to generate rectified currents aligned with the topographic contours (sometimes referred to as the Neptune effect) [*Holloway*, 1992; *Adcock and Marshall*, 1999], somewhat analogous to β-induced rectification (section 3.6). It seems likely that the Neptune effect will generate primarily abyssal currents in the interior and on continental slopes, as they arise from bottom eddies in contact with the topography, but the theoretical basis for predicting their vertical structure is still rudimentary [*Merryfield and Holloway*, 1999].

3.12. Eddy Pumping and Quenching

In many places phytoplankton growth is limited by the supply of nutrients from the oceanic interior into the euphotic zone, and the cycle of plankton consumption and senescence is a biological pump exporting biogeochemical materials into the oceanic interior. Eddy fluxes can contribute to these exchanges through large-scale subduction and ventilation (section 3.8) and mesoscale and submesoscale secondary circulation near fronts (section 3.10). Eddy pumping may also contribute [*Falkowski et al*., 1991; *McGillicuddy and Robinson*, 1997; *Benitez-Nelson et al*., 2007] when the pycnocline is geostrophically elevated inside cyclonic eddies and brings its resident nutrients closer to the surface so growth and cycling can occur. After growth depletes the local nutrients, they can be replenished by isopycnal eddy material fluxes from adjacent regions. Another process is eddy quenching in the biologically active, subtropical eastern boundary upwelling currents where offshore eddy subduction along descending isopycnals removes nutrients from the euphotic zone before plankton growth fully depletes them (Gruber et al., Eddy-induced reduction of biological productivity in upwelling systems, submitted to *Nature*, 2007).

3.13. Eddy-Induced Climate Variability

As eddy effects are an essential part of the dynamics of the large-scale circulation, it can be expected that they will modulate the oceanic variability induced by climate variability in the surface forcing. However, eddies may also be a source of intrinsic climate variability by modifying the large-scale circulation, hence the surface temperature field, hence air-sea fluxes, hence climate. The first stage of this sequence is demonstrated in idealized wind-gyre models with conspicuously high grid resolution and large Reynolds number [*Berloff and McWilliams*, 1999; *Berloff et al*., 2007]: Even with a steady wind stress forcing, the basin-scale circulation changes significantly on decadal time scales, modulated by the eddy fluxes in the separated boundary-current extension and recirculation regions. An analogous spontaneous decadal variability also occurs in the Antarctic Circumpolar Current, albeit by a different mechanism involving eddies and topography [*Hogg and Blundell*, 2006]. As yet, OGCMs and global climate models have not been configured to examine how important this effect might be. Nor have some of the other major current systems—equatorial currents, thermohaline circulation, etc.—yet been investigated for this behavior.

4. CONCLUSIONS

Eddy processes and eddy fluxes have many potential consequences for the oceanic general circulation and climate. The evolution in oceanic modeling toward routinely including eddies through finer scale grid resolution is therefore a significant advance. At present, there are many theoretical ideas and idealized computational demonstrations of eddy effects on the large-scale circulation and material distributions and on climate, but as yet few certainties about how they occur in the real ocean and how they will manifest in more realistic OGCM simulations. Nevertheless, it is now technically feasible to systematically carry out the research that should resolve these uncertainties within the coming years.

Acknowledgments. I am grateful to Pavel Berloff, Bill Dewar, and John Marshall for helpful suggestions about this essay.

Notes

1. More precisely, advection can stir material fields, irreversibly entangle their iso-surfaces, and transfer fluctuation variance to ever-finer scales, but only molecular diffusion can complete the mixing process that ultimately removes the variance of material gradients.
2. A common view is that diapycnal material mixing rates in the pycnocline are mostly due to breaking internal gravity waves [*Gregg*, 1989]. The associated κ value is $\sim 10^{-5}$ m^2 s^{-1}, which is 8 orders of magnitude smaller than the mesoscale isopycnal value above. The extreme anisotropy and disparity of mesoscale and microscale mixing efficiencies are the bases for the quasi-adiabatic hypothesis for eddy material fluxes [*Redi*, 1982; *Gent and McWilliams*, 1990].
3. There is an alternative view that the most useful definition of the eddy-induced transport velocity should be based on the material conservation of potential vorticity and its eddy flux, $\langle v'q' \rangle$, rather than buoyancy as in (5). The differences between these velocities are often small in large-scale flows, as b variations are often the dominant influence in q variations, and the present evidence is mixed about which perspective is preferable [*Marshall et al*., 1999; *Drijfhout and Hazeleger*, 2001].
4. This is also sometimes called the residual mean flow, following *Andrews and McIntyre* [1976], although there are subtle distinctions between these quantities based on the averaging operators.

REFERENCES

Adcock, S. T., and D. P. Marshall (2000), Interactions between geostrophic eddies and the mean circulation over large-scale bottom topography, *J. Phys. Oceanogr.*, *30*, 3223–3238.

Andrews, D. G., and M. McIntyre (1976), Planetary waves in horizontal and vertical shear: The generalized Eliassen-Palm relation and the mean zonal acceleration, *J. Atmos. Sci.*, *33*, 2041–2048.

Armi, L. (1978), Some evidence for boundary mixing in the deep ocean, *J. Geophys. Res.*, *83*, 1971–1979.

Benitz-Nelson, C. R. et al. (2007), Mesoscale eddies drive increased silica export in the Subtropical Pacific Ocean, *Science*, *316*, 1017–1021.

Berloff, P. S., and J. C. McWilliams (1999), Large-scale, low-frequency variability in wind-driven ocean gyres, *J. Phys. Oceanogr.*, *29*, 1925–1949.

Berloff, P. S. (2005), On rectification of randomly forced flows, *J. Mar. Res.*, *63*, 497–527.

Berloff, P., A. Hogg, and W. Dewar (2007), The turbulent oscillator: A mechanism of low-frequency variability of the wind-driven ocean gyres, *J. Phys. Oceanogr.*, *37*, 2363–2386.

Boccaletti, G., R. Ferrari, and B. Fox-Kemper (2007), Mixed layer instabilities and restratification, *J. Phys. Oceanogr.*, *37*, 2228–2250.

Capet, X., J. C. McWilliams, M. J. Molemaker, and A. Shchepetkin (2008a), Mesoscale to submesoscale transition in the California Current System: (I) Flow structure, eddy flux, and observational tests. (II) Frontal processes. (III) Energy balance and flux, *J. Phys. Oceanogr.*, in press.

Capet, X., P. Klein, B. L. Hua, G. Lapeyre, and J. C. McWilliams (2008b), Surface kinetic energy transfer in SQG flows, *J. Fluid Mech.*, in press.

Cessi, P., and M. Fantini (2004), The eddy-driven thermocline, *J. Phys. Oceanogr.*, *34*, 2642–2658.

Charney, J. G. (1971), Geostrophic turbulence, *J. Atmos. Sci.*, *28*, 1087–1095.

Chelton, D. B., M. G. Schlax, R. M. Samelson, and R. A. deSzoeke (2007), Global observations of large oceanic eddies, *Geophys. Res. Lett.*, *34*, L15606, doi:10.1029/2007GL030812.

Dewar, W. K., and J. M. Bane (1985), The subsurface energetics of the Gulf Stream near the Charleston bump, *J. Phys. Oceanogr.*, *15*, 1771–1789.

Drijfhout, S. S., and W. Hazeleger (2001), Eddy mixing of potential vorticity versus thickness in an isopycnic ocean model, *J. Phys. Oceanogr.*, *31*, 481–505.

Ducet, N., P. Y. Le Traeon, and G. Reverdin (2000), Global high-resolution mapping of ocean circulation from TOPEX/Poseidon and ERS-1 and -2, *J. Geophys. Res.*, *105*, 19,477–19,498.

Falkowski, P. G., D. Ziemann, Z. Kolber, and P. K. Bienfang (1991), Role of eddy pumping in enhancing primary production in the ocean, *Nature*, *352*, 55–58.

Ferrari, R., J. C. McWilliams, V. Canuto, and M. Dubovikov (2008), Parameterization of eddy fluxes near oceanic boundaries, *J. Clim.*, in press.

Garrett, C. (1979), Comments on "Some evidence for boundary mixing in the deep ocean" by L. Armi, *J. Geophys. Res.*, *84*, 5095–5096.

Gent, P. R., and J. C. McWilliams (1990), Isopycnal mixing in ocean circulation models, *J. Phys. Oceanogr.*, *20*, 150–155.

Gent, P. R., J. Willebrand, T. J. McDougall, and J. C. McWilliams (1995), Parameterizing eddy-induced tracer transports in ocean circulation models, *J. Phys. Oceanogr.*, *25*, 463–474.

Gill, A. E., J. S. A. Green, and A. J. Simmons (1974), Energy partition in the large-scale ocean circulation and the production of mid-ocean eddies, *Deep-Sea Res.*, *21*, 499–528.

Gregg, M. C. (1989), Scaling turbulent dissipation in the thermocline, *J. Geophys. Res.*, *94*, 9686–9698.

Griffies, S. (1998), The Gent-McWilliams skew flux, *J. Phys. Oceanogr.*, *28*, 831–841.

Haidvogel, D. B., and P. B. Rhines (1983), Waves and circulation driven by oscillatory winds in an idealized ocean basin, *Geophys. Astrophys. Fluid Dyn.*, *25*, 1–63.

Hazeleger, W., and S. S. Drijfhout (2000), Eddy subduction in a model of the subtropical gyre, *J. Phys. Oceanogr.*, *30*, 677–695.

Held, I., R. Pierrehumbert, S. Garner, and K. Swanson (1995), Surface quasigeostrophic dynamics, *J. Fluid Mech.*, *282*, 1–20.

Hogg, A. M., and J. R. Blundell (2006), Interdecadal variability of the Southern Ocean, *J. Phys. Oceanogr.*, *36*, 1626–1645.

Holloway, G. (1992), Representing topographic stress for large-scale ocean models, *J. Phys. Oceanogr.*, *22*, 1033–1046.

Hoskins, B. J., and F. P. Bretherton (1972), Atmospheric frontogenesis models: Mathematical formulation and solution, *J. Atmos. Sci.*, *29*, 11–37.

Hurlburt, H. E., and J. D. Thompson (1980), A numerical study of Loop Current intrusions and eddy shedding, *J. Phys. Oceanogr.*, *10*, 1611–1651.

Jones, H., and J. Marshall (1997), Restratification after deep convection, *J. Phys. Oceanogr.*, *27*, 2276–2287.

Katsman, C. A., M. A. Spall, and R. S. Pickart (2004), Boundary current eddies and their role in the restratification of the Labrador Sea, *J. Phys. Oceanogr.*, *34*, 1967–1983.

Krauss, W., and C. Böning (1987), Lagrangian properties of eddy fields in the northern North Atlantic as deduced from satellite-tracked buoys. *J. Mar. Res.*, *45*, 259–291.

Larichev, V. D., and I. M. Held (1995), Eddy amplitudes and fluxes in a homogeneous model of fully developed baroclinic instability, *J. Phys. Oceanogr.*, *25*, 2285–2297.

Marshall, D. P. (1997), Subduction of water masses in an eddying ocean, *J. Mar. Res.*, *55*, 201–222.

Marshall, D. P., R. G. Williams, and M. M. Lee (1999), The relation between eddy-induced transport and isopycnic gradients of potential vorticity, *J. Phys. Oceanogr.*, *29*, 1571–1578.

Marshall, J. C. (1981), On the parameterization of geostrophic eddies in the ocean, *J. Phys. Oceanogr.*, *11*, 257–271.

Marshall, J. C., H. Jones, R. Karsten, and R. Wardle (2002), Can eddies set ocean stratification?, *J. Phys. Oceanogr.*, *32*, 26–38.

Marshall, J. C., and T. Radko (2003), Residual mean solutions for the Antarctic Circumpolar Current and its associated overturning circulation, *J. Phys. Ocean.*, *33*, 2341–2354.

McGillicuddy, D. J., and A. R. Robinson (1997), Eddy-induced nutrient supply and new production in the Sargasso Sea, *Deep-Sea Res. I*, *44*, 1427–1449.

McWilliams, J. C., and J. H. S. Chow (1981), Equilibrium geostrophic turbulence: I. A reference solution in a beta-plane channel, *J. Phys. Oceanogr.*, *11*, 921–949.

McWilliams, J. C. (1985), Submesoscale, coherent vortices in the ocean, *Rev. Geophys.*, *23*, 165–182.

McWilliams, J. C. (1996), Modeling the oceanic general circulation. *Annu. Rev. Fluid Mech.*, *28*, 1–34.

McWilliams, J. C. (2006), *Fundamentals of Geophysical Fluid Dynamics*, Cambridge University Press, Cambridge, 249 pp.

Merryfield, W. J., and G. Holloway, (1999), Eddy fluxes and topography in stratified quasigeostrophic models, *J. Fluid Mech.*, *380*, 59–80.

Muller, P., J. C. McWilliams, and M. J. Molemaker (2005), Routes to dissipation in the ocean: The 2D/3D turbulence conundrum, in *Marine Turbulence: Theories, Observations and Models*, edited by H. Baumert, J. Simpson, and J. Sundermann, pp. 397–405, Cambridge University Press, Cambridge.

Munk, W. H. (1950), On the wind-driven ocean circulation, *J. Meteorol.*, *7*, 79–93.

Olbers, D., and M. Visbeck (2005), A model of the zonally averaged stratification and overturning in the Southern Ocean, *J. Phys. Oceanogr.*, *35*, 1190–1205.

Pedlosky, J. (1987), *Geophysical Fluid Dynamics*, Springer, New York, 710 pp.

Pope, S. B. (2000), *Turbulent Flows*, Cambridge University Press, Cambridge, 771 pp.

Redi, M. H. (1982), Oceanic isopycnal mixing by coordinate rotation, *J. Phys. Oceanogr.*, *12*, 1154–1158.

Rhines, P. B. (1975), Waves and turbulence on a beta-plane, *J. Fluid Mech.*, *69*, 417–443.

Rhines, P. B., and W. R. Young (1982), Homogenization of potential vorticity in planetary gyres, *J. Fluid Mech.*, *122*, 347–367.

Rudnick, D., and R. Ferrari (1999), Compensation of horizontal temperature and salinity gradients in the ocean mixed layer, *Science*, *283*, 526–529.

Salmon, R. (1982), Geostrophic turbulence, *Topics in Ocean Physics*, Proc. Int. Sch. Phys. 'Enrico Fermi,' Varenna, Italy, pp. 30–78.

Scott, R. B., and F. Wang (2005), Direct evidence of an oceanic inverse kinetic energy cascade from satellite altimetry, *J. Phys. Oceanogr.*, *35*, 1650–1666.

Stammer, D. (1997), Global characteristics of ocean variability estimated from regional TOPEX/POSEIDON altimeter measurements, *J. Phys. Oceanogr.*, *27*, 1743–1769.

Sturges, W., and R. Leben (2000), Frequency of ring separations from the loop current in the Gulf of Mexico: A revised estimate, *J. Phys. Oceanogr.*, *30*, 1814–1819.

Sundermeyer, M., and J. Price (1998), Lateral mixing and the North Atlantic Tracer Release Experiment: Observations and numerical simulations of Lagrangian particles and a passive tracer, *J. Geophys. Res.*, *103*, 21481–21497.

Tai, C. K., and W. B. White (1990), Eddy variability in the Kuroshio Extension as revealed by Geosat Altimetry: Energy propagation away from the jet, Reynolds stress, and seasonal cycle, *J. Phys. Oceanogr.*, *20*, 1761–1777.

Tandon, A., and C. Garrett (1996), On a recent parameterization of mesoscale eddies, *J. Phys. Oceanogr.*, *26*, 406–411.

Thomas, L. N., A. Tandon, and A. Mahadevan (2007), Submesoscale processes and dynamics, this volume.

Treguier, A. M., and J. C. McWilliams (1990), Topographic influences on wind-driven, stratified flow in a β-plane channel: An idealized model of the Antarctic Circumpolar Current, *J. Phys. Oceanogr.*, *20*, 324–343.

Vallis, G. K. (2006), *Atmospheric and Oceanic Fluid Dynamics: Fundamentals and Large-Scale Circulation*, Cambridge University Press, Cambridge, 745 pp.

Wolff, J. O., E. Maier-Reimer, and D. J. Olbers (1991), Wind-driven flow over topography in a zonal β-plane channel: A quasigeostrophic model of the Antarctic Circumpolar Current, *J. Phys. Oceanogr.*, *21*, 236–264.

Wunsch, C., and D. Stammer (1995), The global frequency-wavenumber spectrum of oceanic variability estimated from TOPEX/POSEIDON altimetric measurements, *J. Geophys. Res.*, *100*, 24895–24910.

Wunsch, C., and R. Ferrari (2004), Vertical mixing, energy, and the general circulation of the oceans, *Annu. Rev. Fluid Mech.*, *36*, 281–314.

J. C. McWilliams, Department of Atmospheric and Oceanic Sciences, University of California, Los Angeles, CA, 90095-1565, USA. (jcm@atmos.ucla.edu)

Submesoscale Processes and Dynamics

Leif N. Thomas

Woods Hole Oceanographic Institution, Woods Hole, Massachusetts, USA

Amit Tandon

Physics Department and Department of Estuarine and Ocean Sciences, University of Massachusetts, Dartmouth, North Dartmouth, Massachusetts, USA

Amala Mahadevan

Department of Earth Sciences, Boston University, Boston, Massachusetts, USA

Increased spatial resolution in recent observations and modeling has revealed a richness of structure and processes on lateral scales of a kilometer in the upper ocean. Processes at this scale, termed submesoscale, are distinguished by order-one ($O(1)$) Rossby and Richardson numbers; their dynamics are distinct from those of the largely quasi-geostrophic mesoscale as well as fully three-dimensional, small-scale processes. Submesoscale processes make an important contribution to the vertical flux of mass, buoyancy, and tracers in the upper ocean. They flux potential vorticity through the mixed layer, enhance communication between the pycnocline and surface, and play a crucial role in changing the upper-ocean stratification and mixed-layer structure on a timescale of days. In this review, we present a synthesis of upper-ocean submesoscale processes that arise in the presence of lateral buoyancy gradients. We describe their generation through frontogenesis, unforced instabilities, and forced motions due to buoyancy loss or down-front winds. Using the semi-geostrophic (SG) framework, we present physical arguments to help interpret several key aspects of submesoscale flows. These include the development of narrow elongated regions with $O(1)$ Rossby and Richardson numbers through frontogenesis, intense vertical velocities with a downward bias at these sites, and secondary circulations that redistribute buoyancy to stratify the mixed layer. We review some of the first parameterizations for submesoscale processes that attempt to capture their contribution to, first, vertical buoyancy fluxes and restratification by mixed-layer instabilities and, second, the exchange of potential vorticity between the wind- and buoyancy-forced surface mixed layer, and pycnocline. Submesoscale processes are emerging as vital for the transport of biogeochemical properties, for

Ocean Modeling in an Eddying Regime
Geophysical Monograph Series 177

10.1029/177GM04

generating spatial heterogeneity that is critical for biogeochemical processes and mixing, and for the transfer of energy from meso- to small scales. Several studies are in progress to model, measure, analyze, understand, and parameterize these motions.

1. INTRODUCTION

The oceanic mesoscale flow field, characterized by a horizontal length scale of 10 to 100 km, has been studied extensively for its dynamics and its contribution to the lateral transport of heat, momentum, and tracers by means of eddies. Similarly, three-dimensional processes at small lengthscales less than a kilometer (0.1–100 m) have been investigated for their contribution to mixing and energy dissipation. However, submesoscales (~1 km) that lie intermediate to meso- and small-scale three-dimensional motions are less understood and have only more recently been brought to light through observational, modeling, and analytical studies. The submesoscale, characterized by $\mathcal{O}(1)$ Rossby number dynamics, is not described appropriately by the traditional quasi-geostrophic theory that applies to mesoscales. It is not fully three-dimensional and nonhydrostatic, either, but is inevitably crucial to bridging the meso- and smaller scales through processes and dynamics that we are just beginning to understand. The objective of this article was to review and synthesize the understanding of submesoscales put forth through recent diverse studies.

Our discussion will focus on the upper ocean where submesoscale processes are particularly dominant due to the presence of lateral density gradients, vertical shear, weak stratification, a surface boundary that is conducive to frontogenesis, and a relatively small Rossby radius based on the mixed-layer depth. This is not to say that submesoscale phenomenon occurs solely in the upper ocean. In the ocean interior and abyss, there are submesoscale coherent vortices [*McWilliams*, 1985] and balanced flows associated with the oceanic vortical mode, which are thought to play an important role in the isopycnal stirring of tracers [*Kunze and Stanford*, 1993; *Kunze*, 2001; *Polzin and Ferrari*, 2003; *Sundermeyer and Lelong*, 2005]. Furthermore, internal gravity waves can vary on the submesoscale, but will not be described in this review.

The motivation to study submesoscale processes comes from several factors. As the geometrical aspect (depth to length) ratio and Rossby number *Ro*, associated with meso- and larger scale flow are $\ll 1$, and the Richardson number $Ri \gg 1$, the associated vertical velocities are 10^{-3} to 10^{-4} times smaller than the horizontal velocities, which are typically 0.1 m s^{-1}. However, localized submesoscale regions develop in which *Ro* and *Ri* are $O(1)$. At these sites, submesoscale dynamics generate vertical velocities of $O(10^{-3})$ m s^{-1} or ~ 100 m day^{-1} that are typically an order of magnitude larger than those associated with the mesoscale. In addition, at the submesoscale, there is a marked asymmetry in the strength of upwelling versus downwelling and anticyclonic versus cyclonic vorticity, with an enhancement of downward velocity and cyclonic vorticity.

Owing to their large vertical velocities, submesoscale processes can be instrumental in transferring properties and tracers, vertically, between the surface ocean and the interior. This vertical transport plays an important role in supplying nutrients to the euphotic zone for phytoplankton production and exchanging gases between the atmosphere and the ocean. Understanding how vertical exchange is achieved between the biologically active, but nutrient-depleted, surface euphotic layer and the nutrient-replete thermocline has been a long-standing question for the carbon cycle and biogeochemistry of the upper ocean. For example, estimates of new production (phytoplankton production relying on a fresh rather than recycled supply of nutrients) based on oxygen utilization and cycling rates [*Platt and Harrison*, 1985; *Jenkins and Goldman*, 1985; *Emerson et al*., 1997] and helium fluxes [*Jenkins*, 1988] are much higher in the subtropical gyres than can be accounted for through the physical circulation in global carbon cycle models [*Najjar et al*., 1992; *Maier-Reimer*, 1993]. Several studies, such as those of *McGillicuddy and Robinson* [1997] and *McGillicuddy et al*. [1998], suggest that mesoscale eddies act to pump nutrients to the euphotic zone. However, a basinwide estimate for the eddy-pumping fluxes [*Oschlies*, 2002a; *Martin and Pondaven*, 2003; *Oschlies*, 2007] turns out to be inadequate in supplying the nutrient flux required to sustain the observed levels of productivity in the subtropical gyres. As described above, vertical velocities associated with submesoscale features are much stronger than their mesoscale counterparts, suggesting that submesoscale vertical fluxes of nutrients may play a critical role in enhancing productivity not only in the subtropical gyres but in the world ocean as a whole.

A large part of the ocean's kinetic energy resides at meso- and larger scales. At these scales, oceanic flow is largely two-dimensional and in a state of hydrostatic and geostrophic balance from which it is difficult to extract energy.

A major conundrum [*McWilliams et al*., 2001; *McWilliams*, 2003], therefore, is how energy is transferred from the mesoscale to the small scale at which it can be dissipated through three-dimensional processes. The strong ageostrophic flow at submesoscales can extract energy from the balanced state and transfer it to smaller scales. *Charney* [1971] argued that large-scale stirring would induce a forward enstrophy cascade consistent with a kinetic energy spectrum of slope −3. For the oceanic context, numerical simulations have shown that the quasi two-dimensional mesoscale flow field is characterized by kinetic energy spectra with a slope of −3 [*Capet et al*., 2008a; *Klein et al.*, 2007]. Three-dimensional numerical simulations at progressively finer resolutions show that resolving submesoscale processes leads to flattening the kinetic energy spectra slope to −2 [*Capet et al*., 2008a] and a transfer of energy to larger as well as smaller scales [*Boccaletti et al*., 2007].

Yet, another factor associated with submesoscale instabilities is the flux of potential vorticity to and from the surface to the interior ocean and the change in stratification of the mixed layer. Submesoscale instabilities in the mixed layer are shown to hasten restratification and buoyancy transport several-fold as compared to what can be achieved through mesoscale baroclinic instability [*Fox-Kemper et al.*, 2007]. Hence, their contribution to eddy transport can be significant. Present-day global circulation models do not resolve submesocales; conceivably, this is the reason for the dearth of restratifying processes and mixed layers that are far too deep in the models [*Oschlies*, 2002b; *Hallberg*, 2003; *Fox-Kemper et al.*, 2007]. Hence, parameterizing these processes is of interest to climate modeling. Similarly, the cumulative vertical flux of potential vorticity through submesoscale processes can alter the potential vorticity budget of the thermocline and mixed layer [*Thomas*, 2005, 2007]. Submesoscale dynamics provide a pathway between the surface boundary layer, where properties are changed by friction and diabatic processes, and the interior, which is largely adiabatic and conserves properties.

Resolving submesoscales within the mesoscale field has been a challenge for models and observations, but one that is being currently met through improvements in technology. Hydrographic surveys using towed vehicles (such as a SeaSoar) equipped with conductivity-temperature-depth sensors have revealed submesoscale features in the upper ocean associated with compensated and uncompensated ocean fronts [e.g., *Pollard and Regier*, 1992; *Rudnick and Luyten*, 1996; *Rudnick and Ferrari*, 1999; *Lee et al*., 2006b]. Shipboard acoustic Doppler current profiler velocity measurements show that the distribution of the relative vorticity in the upper ocean is skewed to positive values, hinting at the presence of submesoscale flows with stronger cyclonic versus anticyclonic vorticity [*Rudnick*, 2001]. Recent observations centered around a drifter show the role played by the baroclinicity in setting the stratification within the mixed layer (Hosegood et al., Restratification of the surface mixed layer with submesoscale lateral gradients: Diagnosing the importance of the horizontal dimension, submitted to *Journal of Physical Oceanography*, 2007). Similar measurements made following mixed-layer Lagrangian floats have captured rapid (occurring over a day) changes in the mixed-layer stratification that cannot be ascribed to heating or cooling, and hence, are thought to result from submesoscale processes [*Lee et al*., 2006a]. Further examples of submesoscale variability are seen in high-resolution velocity fields from radar [*Shay et al*., 2003], sea-surface temperature fields from satellites [*Flament et al*., 1985; *Capet et al*., 2008b], a proliferation of cyclonic vortices revealed by sunglitter on the sea surface [*Munk et al*., 2000], and biogeochemical sampling along ship transects. We are at an exciting juncture because we are now able to achieve the required resolution in models and observations to capture this scale. The results from high-resolution numerical modeling and analytical studies, several of which are discussed in this review, suggest that both forced and unforced instabilities drive submesoscale processes.

We begin section 2 by defining the term submesoscale and describing phenomena with which it is associated. Furthermore, we examine mechanisms that generate submesoscales in the upper ocean. In section 3, we present a mathematical framework for understanding the secondary circulation associated with fronts where submesoscale processes are found to be active. This framework is used to provide a dynamical explanation for several key features of submesoscale phenomena. In section 4, we discuss the implications of submesoscale phenomena, which include mixed-layer restratification, vertical transport and biogeochemical fluxes, and potential vorticity fluxes. Finally, we provide a discussion of outstanding questions and possible connections to other areas.

2. PHENOMENOLOGY

2.1. What are Submesoscales?

An active flow field in the upper ocean generates localized regions, typically along filaments or outcropping isopycnals, within which the relative vertical vorticity $\zeta = v_x - u_y$ equals or exceeds the planetary vorticity f, and the vertical shear can be quite strong. The dynamics within these regions differs from mesoscale dynamics characterized by small Rossby numbers ($Ro \ll 1$) and large Richardson numbers ($Ri \gg 1$). We thus define submesoscale flows

based on dynamics, as those where the gradient Rossby number, $Ro = |\zeta|/f$, and the gradient Richardson number, $Ri = N^2/|\partial_z \mathbf{u}_h|^2$, are both $\mathcal{O}(1)$, where $\mathbf{u}_h$ is the horizontal velocity, $N^2 = b_z$ is the square of the buoyancy frequency, $b = -g\rho/\rho_o$ is the buoyancy, ρ is the density, g is the acceleration due to gravity, and ρ_o is a reference density. If we introduce bulk Richardson and Rossby numbers: $Ri_b = N^2H^2/U^2$ and $Ro_b = U/fL$ (U, H, and L are the characteristic speed, vertical lengthscale, and horizontal lengthscale of the velocity field, respectively), it then follows that submesoscale flows with $Ro_b = Ri_b = \mathcal{O}(1)$ are also characterized by an order-one Burger number $Bu = N^2H^2/f^2L^2$. It is worth noting that the bulk Richardson number can be related to the Froude number $Fr = U/NH = 1/\sqrt{Ri_b}$. Submesoscale flows, as we define them here, are hence characterized by $Fr \geq 1$. This parameter range with $Ro_b = \mathcal{O}(1)$ is also relevant to the transition from geostrophic to stratified turbulence [e.g., *Waite and Bartello*, 2006].

The characteristic vertical extent H of upper-ocean submesoscale phenomena typically scales with the mixed-layer depth h_{ml}. The condition that $Bu \sim 1$ implies that the horizontal lengthscale associated with submesoscale processes scales with the mixed-layer Rossby radius of deformation

$$L \sim L_{ml} = \frac{N_{ml} h_{ml}}{f}, \tag{1}$$

where N_{ml} is the buoyancy frequency in the mixed layer. The weak stratification and limited vertical extent of mixed layers makes the characteristic length of submesoscale flows small relative to the first baroclinic Rossby radius of deformation that defines the mesoscale. For example, a mixed layer of depth $h_{ml} = 100$ m, with $N_{ml} = 10^{-3}$ s^{-1} in the mid-latitudes ($f = 1 \times 10^{-4}$ s^{-1}), yields $L \sim L_{ml} = 1$ km. Given this small horizontal scale, it only takes a relatively weak velocity of $U = 0.1$ m s^{-1} to yield a Rossby number of order-one, indicating that such modest submesoscale flows can be susceptible to nonlinear dynamics and ageostrophic effects.

Another way to state the $Bu = 1$ condition is that the aspect ratio of submesoscale flows, $\Gamma = H/L$, scales as f/N. For typical oceanic conditions, $f/N \ll 1$, so that $\Gamma \ll 1$. Scaling the vertical momentum equation shows that the hydrostatic balance is accurate to $O(Ro^2\,\Gamma)$. Hence, although $Ro = \mathcal{O}(1)$ for submesoscale flows, $\Gamma \ll 1$ in the upper ocean, and these processes can, to a good approximation, be considered hydrostatic. Indeed, non-hydrostatic effects are difficult to detect in submesoscale model simulations at horizontal grid resolutions of 500 m [*Mahadevan*, 2006].

Another perspective used to understand submesocale processes is in terms of Ertel's potential vorticity (PV)

$$q = (f + \zeta)N^2 + \omega_h \cdot \nabla_h b, \tag{2}$$

where $\omega_h = (w_y - v_z,\, u_z - w_x)$ is the horizontal vorticity and $\nabla_h b$ is the horizontal buoyancy gradient. At large scales and in the interior, q is dominated by the planetary PV: fN^2. At mesoscales, the contribution from the vertical vorticity, ζN^2, becomes important. In the upper ocean, in the presence of density gradients arising from frontal filaments or outcropping isopycnals, the contribution to q from the horizontal buoyancy gradient and the thermal wind shear $(u_z^{tw}, v_z^{tw}) = (-b_y/f, b_x/f)$ becomes important and always tends to lower the PV. More specifically, the contribution to the PV from horizontal buoyancy gradients is as large as the planetary PV and significantly reduces the magnitude of the total PV when the Richardson number is $\mathcal{O}(1)$, that is, when the flow is submesoscale according to our dynamical definition [*Tandon and Garrett*, 1994; *Thomas*, 2007]. Submesoscale dynamics are thus intimately linked with processes that modify the PV, such as forcing by wind stress and buoyancy fluxes and advection of PV by eddies. This chapter therefore often uses PV as a means to help interpret submesoscale physics.

Next, we describe mechanisms that are known to be active in generating submesoscales including (1) frontogenesis; (2) unforced instabilities, such as the ageostrophic baroclinic instability [*Molemaker et al*., 2005; *Boccaletti et al*., 2007]; and (3) forced motion, such as flows affected by buoyancy fluxes or friction at boundaries. We will use the results from a numerical model to individually demonstrate the above submesoscale mechanisms. Although the submesoscale conditions are localized in space and time, the mesoscale flow field is crucial in generating them. In the ocean, it is likely that more than one submesoscale mechanism acts in tandem with mesoscale dynamics to produce a complex submesoscale structure within the fabric of the mesoscale flow field.

2.2. Frontogenesis

Consider the flow field generated by a geostrophically balanced front in the upper mixed layer of the ocean overlying a pycnocline. As the front becomes unstable and meanders, the nonlinear interaction of the lateral velocity shear and buoyancy gradient locally intensify the across-front buoyancy gradient. Strong frontogenetic action pinches outcropping isopycnals together, generating narrow regions in which the lateral shear and relative vorticity become very large, and the Ro and Ri become $\mathcal{O}(1)$. At these sites, the lateral strain rate $S \equiv ((u_x - v_y)^2 + (v_x - u_y)^2)^{1/2}$ is also large, and strong ageostrophic overturning circulation generates intense vertical velocities. In Figure 1, we plot the density, horizontal and vertical velocities, strain rate, Ro, and Ri from a frontal region in a model simulation. The model was initialized with an across-front density variation of 0.27 kg m^{-3}

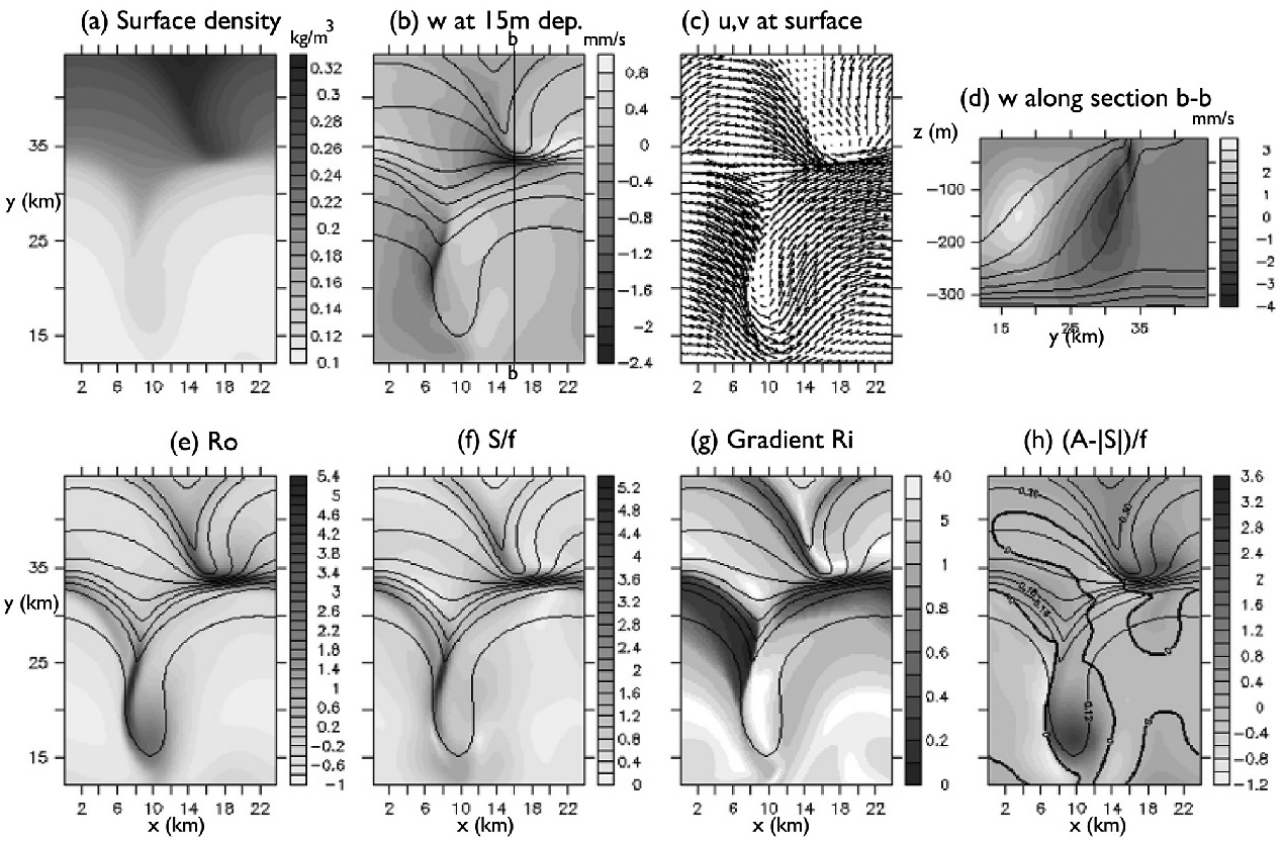

Figure 1. A region in the model domain where spontaneous frontogenesis has set up large shear and relative vorticity ζ, high lateral strain rate *S*, and a strong ageostrophic secondary circulation. (a) Surface density, (b) vertical velocity at 15 m depth, (c) surface *u*, *v* velocities, (d) vertical section through the front at $x = 16$ km showing vertical velocity (light tones indicate upward, dark tones downward) and isopycnals (black contours), (e) $Ro = \zeta / f$, (f) S / f, (g) gradient Ri, and (h) $(A - |S|)/f$ with the zero contour shown as a dark black line. Light black contours indicate surface density in all cases.

across 20 km (i.e., $|b_y| \approx 10^{-7}$ s^{-2}), over a deep mixed layer extending to 250 m and allowed to evolve in an east–west periodic channel with solid southern and northern boundaries. Submesoscale frontogenesis is more easily seen when the mixed layer is deep because the horizontal scale, which is dependent on h_{ml}, is larger and more readily resolved in the numerical model. Here, the mixed layer is taken to be 250 m deep so as to exaggerate frontogenesis. As the baroclinically unstable front meanders, the lateral buoyancy gradient is spontaneously locally intensified in certain regions, as in Figure 1, generating submesoscale conditions at sites approximately 5 km in width. This mechanism is ubiquitous to the upper ocean due to the presence of lateral buoyancy gradients and generates submesoscale phenomena when intensification can proceed without excessive frictional damping, or in a model with sufficient numerical resolution and minimal viscosity.

2.3. Unforced Instabilities

The instabilities in the mixed-layer regime where $Ro = \mathcal{O}(1)$ and $Ri = Ro^{-1/2} = \mathcal{O}(1)$ are different from the geostrophic baroclinic mode in several respects. The ageostrophic baroclinic instability problem of a sheared rotating stratified flow in thermal wind balance with a constant horizontal buoyancy gradient was investigated using hydrostatic [*Stone*, 1966, 1970] and non-hydrostatic equations [*Stone*, 1971] for finite values of *Ro*. *Molemaker et al*. [2005] extend these analyses by examining them in the context of loss of balance that leads to a forward energy cascade. Their instability analysis is applicable to the mixed-layer regime and shows two distinct instabilities. The largest growth rates arise for a geostrophic mode (large *Ro* Eady mode), which is mostly balanced and well captured by hydrostatic equations [*Stone*, 1966, 1970]. *Boccaletti et al*. [2007]